Check for updates

View Article Online
View Journal

Chemical Science

Accepted Manuscript

This article can be cited before page numbers have been issued, to do this please use: X. Zhao, L. Liu, Z. Zhang, T. Qin, J. Hu, L. Ying, J. Zhu, T. Wang and X. Miao, *Chem. Sci.*, 2025, DOI: 10.1039/D5SC01269D.

This is an Accepted Manuscript, which has been through the Royal Society of Chemistry peer review process and has been accepted for publication.

Accepted Manuscripts are published online shortly after acceptance, before technical editing, formatting and proof reading. Using this free service, authors can make their results available to the community, in citable form, before we publish the edited article. We will replace this Accepted Manuscript with the edited and formatted Advance Article as soon as it is available.

You can find more information about Accepted Manuscripts in the Information for Authors.

Please note that technical editing may introduce minor changes to the text and/or graphics, which may alter content. The journal's standard Terms & Conditions and the Ethical guidelines still apply. In no event shall the Royal Society of Chemistry be held responsible for any errors or omissions in this Accepted Manuscript or any consequences arising from the use of any information it contains.

ROYAL SOCIETY OF CHEMISTRY

rsc.li/chemical-science

On-surface synthesis of organometallic nanorings linked by unconventional intermediates of Ullmann reaction

View Article Online
DOI: 10.1039/D5SC01269D

Xiaoyang Zhao[†a], Liqian Liu[†a], Zhipeng Zhang[a], Tianchen Qin[b], Jun Hu[b], Lei Ying[a], Junfa Zhu[b], Tao Wang[c*], Xinrui Miao[a*]

[a]State Key Laboratory of Luminescent Materials and Devices, College of Materials Science and Engineering, South China University of Technology, Guangzhou, 510640, P. R. China

[b]National Synchrotron Radiation Laboratory, University of Science and Technology of China, Hefei, 230029, P. R. China

[c]State Key Laboratory of Organometallic Chemistry, Shanghai Institute of Organic Chemistry, Chinese Academy of Sciences, Shanghai, 200032, P. R. China

Corresponding authors: Xinrui Miao (msxrmiao@scut.edu.cn)
Tao Wang (taowang@sioc.ac.cn)

[†] These authors contributed equally.

Abstract: Ullmann coupling has been one of the most important organic reactions for the formation of aryl–aryl bond, which is of great significance in medicinal chemistry, natural product synthesis, and optoelectronic material fabrication. However, the associated reaction mechanism has not been known with certainty and mostly relied on theoretical calculations, since the identification of reaction intermediates lacked of experimental evidences. Herein, we report the visualization of an unprecedented C–Cu–Br–Cu–C bonded intermediate state of Ullmann coupling by means of on-surface synthesis. These intermediates tend to form nanorings on a Cu(111) surface, as the thermodynamically stable structures. The advanced techniques including scanning tunneling microscopy, non-contact atomic force microscopy, synchrotron radiation photoemission spectroscopy, together with density functional theory calculations, scrutinized the structural assignments and intermediate transition process at the sub-molecular level. The C–Cu–Br–Cu–C structure is confirmed to be the precursor state of the conventional C–Cu–C intermediate during on-surface Ullmann reaction, since their coexistence and transformation were observed experimentally. Our findings offer insights into revisiting and understanding reaction mechanism of Ullmann coupling.

Open Access Article. Published on 21 April 2025. Downloaded on 4/24/2025 4:15:25 AM.
This article is licensed under a Creative Commons Attribution-NonCommercial 3.0 Unported Licence.

Chemical Science Accepted Manuscript

View Article Online
DOI: 10.1039/D5SC01269D

Open Access Article. Published on 21 April 2025. Downloaded on 4/24/2025 4:15:25 AM.
This article is licensed under a Creative Commons Attribution-NonCommercial 3.0 Unported Licence.

Introduction

Ullmann coupling has intensely utilized to synthesize symmetrical and asymmetric biphenyl compounds, which has a wide range of applications in medicinal chemistry, materials science, and organic synthesis.[1, 2] Although high reaction efficiency and selectivity have been achieved in the past a few decades, the reaction mechanism of Ullmann coupling remains elusive because the capture and accurate characterization of reaction intermediates are challenging. Consequently, the interpretation of reaction mechanisms of Ullmann coupling largely relied on theoretical calculations. As for the classical metal (M)-catalyzed Ullmann reaction systems, two representative mechanisms rationalized by calculations are single electron transfer mechanism and M(I)-M(III) ionic mechanism.[3] The latter involves more complex pathway and has been more popular (Scheme 1a), in which a M(III) species acts as an important intermediate prior to the final formation of C−C covalent bond (red dashed frame).[4-6] However, although this predicted mechanism could be reasonable for Cu-catalyzed Ullmann coupling (Scheme 1a), it is probably not universal and has been debatable because it is not possible for interpreting the reaction mechanism of Pd or Ni catalyzed Ullmann couplings.[7, 8] Pd(III) and Ni(III) species are not their common valence states, thus different reaction mechanisms in Pd or Ni catalyzed reaction systems have to be proposed. Therefore, the inadequate understanding of reaction mechanism up to date has been a major obstacle for rational design of catalysts and further development of Ullmann coupling. The key for depicting the reaction mechanism of Ullmann coupling is the effective detection and precise characterization of reaction intermediates.

The recently developed on-surface synthesis has provided an unprecedented opportunity for the visualization of reaction intermediates and products at the single-molecule level, with the aid of scanning tunneling microscopy (STM) and non-contact atomic force microscopy (nc-AFM) imaging under ultra-high vacuum condition.[9-13] In addition, the molecule−substrate interaction helps the stabilization and thereof the capture of metastable intermediates.[14, 15] Upon on-surface synthesis approach, the mechanism of several organic reactions has been unraveled at the sub-molecular scale in real space, such as intermolecular radical transfer,[16] ethylene polymerization,[17] nucleation–elongation of boroxine polymer,[18] etc.[19-22] However, as the most widely utilized on-surface reaction for the synthesis of graphene nanoribbons and covalent networks,[23-26] the detailed reaction pathway of on-surface Ullmann coupling has been largely unknown.[27] The only conventionally captured and characterized intermediate is the C−M−C species (M=Au, Ag, Cu; Scheme 1b),[28-30] which transforms into the C−C covalent bond upon further activation. The process starting from C−X (X = Cl, Br, I) dissociation to the formation of C−M−C species, however, is unclear.[31, 32] This is probably attributed to the short life-time of the associated C−M−X or similar intermediates, *i.e.* a negligible energy barrier from C−M−X to C−M−C species.

Note that in solution-phase Ullmann coupling, the introduction of N-containing ligands enables the coupling reaction to proceed under mild conditions.[33-35] Therefore, the N-containing ligands may influence

Chemical Science Accepted Manuscript

View Article Online
DOI: 10.1039/D5SC01269D

Open Access Article. Published on 21 April 2025. Downloaded on 4/24/2025 4:15:25 AM.
This article is licensed under a Creative Commons Attribution-NonCommercial 3.0 Unported Licence.

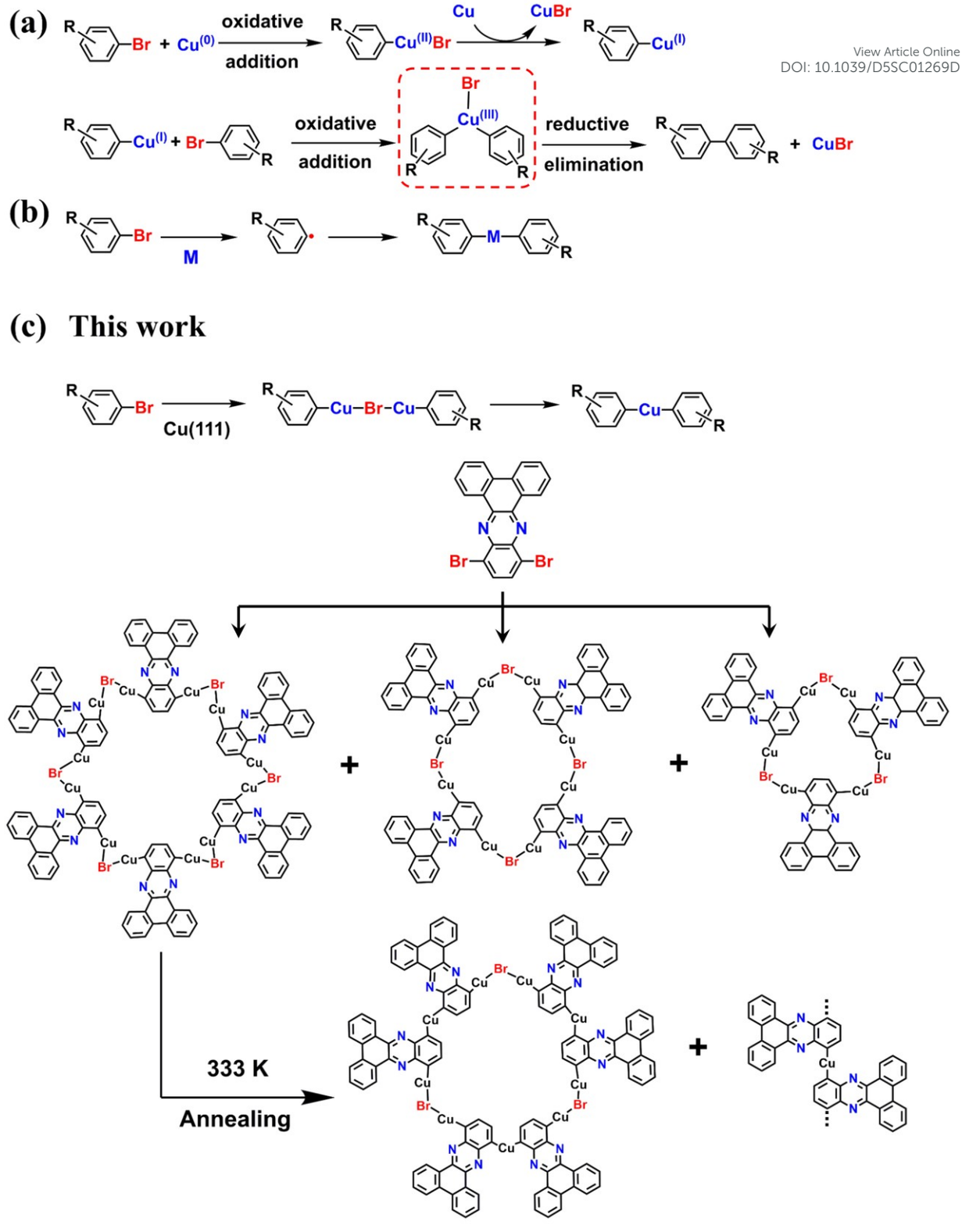

Scheme 1. Schematic illustration of Ullmann coupling reactions. (a) Possible mechanism of Cu-catalyzed Ullmann coupling in-solution chemistry. (b) The conventional reaction pathway of on-surface Ullmann coupling. (c) Reaction pathway of DBP-Br precursor on Cu(111), in which C−Cu−Br−Cu−C bonded nanorings are formed at RT and transform into C−Cu−C bonded nanorings and *trans*-dimer after annealing at 333 K.

Chemical Science Accepted Manuscript

View Article Online
DOI: 10.1039/D5SC01269D

the formation, evolution, and lifetime of intermediates, potentially contributing to the intermediate capture. Inspired by this, herein, we investigated the reaction mechanism of N-doped brominated molecules on a Cu(111) surface by monitoring the formation of organometallic intermediates. 10,13-Dibromodibenzo[a,c]phenazine (DBP-Br) with the phenazine unit close to the brominated benzene ring was used as the precursor. Interestingly, a series of N-doped nanorings were fabricated by depositing of DBP-Br on Cu(111) at room temperature (RT) (Scheme 1c), which are stabilized by unusual C−Cu−Br−Cu−C bonds, as confirmed by the combined STM, nc-AFM, synchrotron radiation photoemission spectroscopy (SRPES), and density functional theory (DFT) calculations. The C–Cu–Br–Cu–C species transformed to the conventional C−Cu−C bond upon further annealing, indicating the former is a precursor state of the latter. We note that the C–Cu–Br–Cu–C bonded intermediate is similar but different as the theoretically possible counterpart in solution-phase Ullmann reaction (red dashed frame in Scheme 1a), which may arouse scientists' interests on revisiting reaction mechanism of solution-phase Ullmann coupling. This work extends the insights on Ullmann coupling mechanism by visualizing diverse reaction intermediates in real space.

Results and Discussion

After depositing DBP-Br molecules with approximately 0.5 monolayer (ML) onto the Cu(111) surface kept at RT, prevailing nanorings were observed unexpectedly (Fig. 1a). 6-Membered rings are the major products and a small amount of 4-membered nanorings (blue circles in Fig. 1a; high-resolution images are seen in Fig. S1) coexist. The zoom-in STM images displayed in Fig. 1b-c reveal the detailed structure of a 6-membered ring composed of six DBP units, in which the "serrations" correspond to the phenanthrene backbones and the quinoxaline groups exhibit as dark "grooves" (Fig. S1). We notice that the distance (~7.6 Å) (Fig. 1c) between adjacent DBP units is remarkably longer than that of the conventional C−Cu−C bond (~3.8 Å)[36, 37] formed after the dissociation of C−Br bonds on Cu(111) at RT. Two dots are resolved in this bond, thus a direct intuition is that the bond might be a C−Cu−Cu−C motif. However, the C−Cu−Cu−C motif is extremely unstable according to DFT calculations, which automatically dissociated during optimization. Inspired by the C−Cu−Br linked intermediates in solution-phase Ullmann coupling,[33, 35] we propose that the bond here may be assigned to C−Cu−Br−Cu−C motif, as supported by the good agreement between DFT simulated STM image/molecular adsorption model and the corresponding experimental results (Fig. 1d-e and S1). According to the calculation, the angle of Cu−Br−Cu bond is about 88° and Br atoms are invisible in the typical range of scanning bias voltage because of their low density of electronic states. We notice that only six Br atoms are required for the formation of a C−Cu−Br−Cu−C linked six-membered nanoring, implying that other six Br atoms provided by the precursors should adsorb on the Cu(111) surface, which are clearly visible in some high-resolution STM images (Fig. S2).[38, 39]

Open Access Article. Published on 21 April 2025. Downloaded on 4/24/2025 4:15:25 AM.
This article is licensed under a Creative Commons Attribution-NonCommercial 3.0 Unported Licence.

Chemical Science Accepted Manuscript

View Article Online
DOI: 10.1039/D5SC01269D

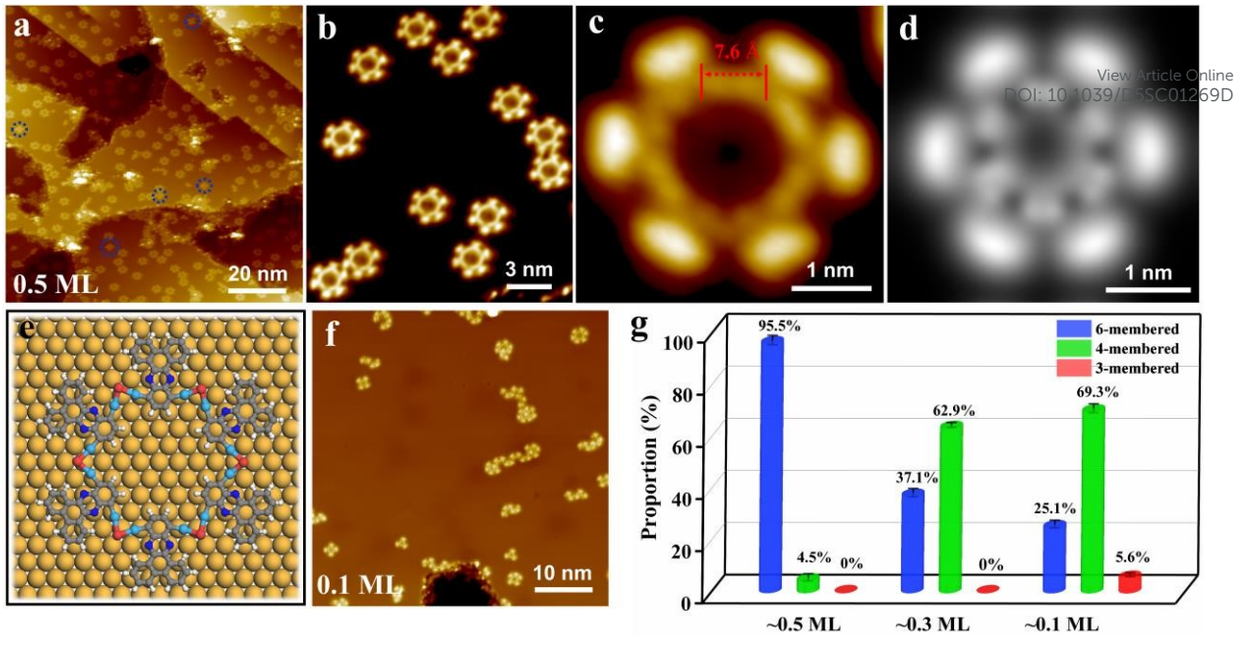

Fig. 1. Characterization of C−Cu−Br−Cu−C bonded nanorings by scanning probe microscopies. (a) Large-scale STM image recorded after depositing DBP-Br with a coverage of 0.5 ML on Cu(111) held at 300 K. (b) Typical STM image showing uniform 6-membered nanorings. (c) Close-up STM image of a single 6-membered nanoring. (d) Simulated STM image of the 6-membered nanoring using a bias voltage of 500 mV. (e) DFT-optimized molecular model of the 6-membered nanoring linked by C−Cu−Br−Cu−C bonds on the Cu(111) surface. (f) Large-scale STM image recorded after depositing DBP-Br with a coverage of 0.1 ML on Cu(111) held at 300 K. (g) Statistical analysis of the observed nanorings with different coverages on Cu(111), by counting more than 650 organometallic nanoring structures on each sample. Scanning parameters: (a−c, f) V_{bias} = 500 mV, I_{set} = 50 pA.

The above organometallic nanorings are linked through a novel C−Cu−Br−Cu−C bond, extending the family of functional organic nanorings. Interestingly, the topology of these nanorings can be tuned by molecular coverage. As shown in Fig. 1f and S3-S5, the dominating nanoring products on Cu(111) at RT evolved from the larger 6-membered ring, to smaller 4- and 3-membered rings, along with the coverage decreasing. In particular, the smallest 3-membered ring,[40] which is difficult to be synthesized on surfaces, starts generating only at an extremely low coverage of 0.1 ML.[36] These nanorings kept their structural integrity even by leaving the sample at RT for four days (Fig. S6), exhibiting a high thermostability.

To investigate intermediate evolution from the unusual C−Cu−Br−Cu−C motif to the conventional C−Cu−C motif of Ullmann coupling on Cu(111), the sample was annealed at 333 K for 20 mins. As shown in the representative STM images (Fig. 2a and Fig. S7-S8), the majority of 6-membered nanorings opened and the morphology of surviving nanorings has changed compared to the original ones in Fig. 1. An example of such 6-membered nanorings is displayed in Fig. 2b-c. While three bonds kept their original configuration as the C−Cu−Br−Cu−C connection, other three bonds became much shorter whose length is measured to be

Open Access Article. Published on 21 April 2025. Downloaded on 4/24/2025 4:15:25 AM.
This article is licensed under a Creative Commons Attribution-NonCommercial 3.0 Unported Licence.

Chemical Science Accepted Manuscript

about 3.8 Å. This strongly implies the short bonds are assigned to the conventional C−Cu−C bonds in Ullmann coupling on Cu(111), where the bright dots correspond to the Cu adatoms.[30] In addition, the majority of the observed *trans*-dimer and chain-like structure formed after ring-opening are also linked by C−Cu−C bonds, as represented by the STM image of *trans*-dimer in Fig. 2d. The chemical structure matches well with the corresponding STM image (Fig. 2e), in which the bright dot is again assigned to Cu adatom and the phenyls binding to Cu shows relatively dark contrast because of their low adsorption height (Fig. S9). Such transformation described above provides direct evidences that the unusual C−Cu−Br−Cu−C intermediate starts evolving into the C−Cu−C motif at this condition. In this process, the nanorings tend to open in order to avoid the large ring tension, noting that the formed C−Cu−C bond (the angle is typically >160°)[41-43] is not possible to bend as a similar angle as that of the Cu−Br−Cu bond (80−90°; Fig. S10) to keep the prefect cyclic geometry.

View Article Online
DOI: 10.1039/D5SC01269D

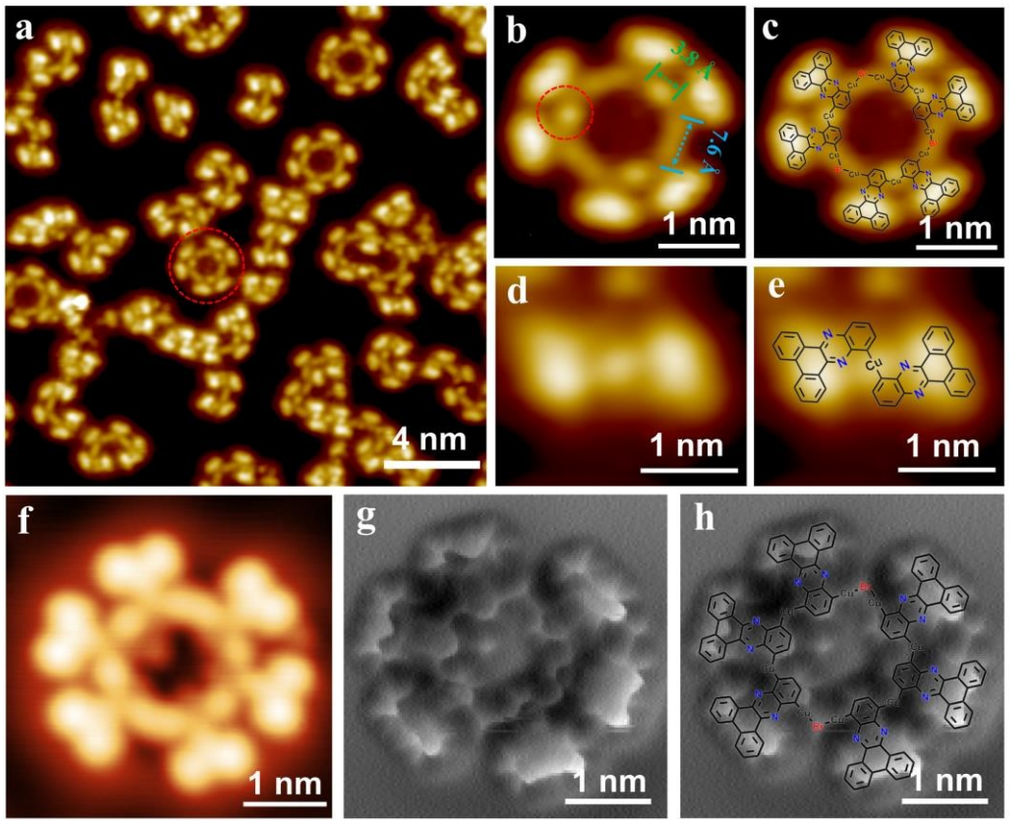

Fig. 2. Transformation between C−Cu−Br−Cu−C to C−Cu−C bonded intermediates and bond-resolving image of C−Cu−Br−Cu−C bonded nanoring. (a) Overview STM image revealing the structural evolution by annealing the sample at 333 K. (b) Zoom-in STM image of a 6-membered ring containing both C−Cu−Br−Cu−C and C−Cu−C bonds. The corresponding chemical structure is overlapped in (c). (d) Zoom-in STM image of a *trans*-dimer. The corresponding chemical structure is overlapped in (e). (f) Representative STM image and (g) nc-AFM image of a 6-membered ring containing both C−Cu−Br−Cu−C and C−Cu−C bonds. The corresponding chemical structure is overlapped in (h). Scanning parameters: (a−c, f) V_{bias} = 500 mV, I_{set} = 50 pA.

Open Access Article. Published on 21 April 2025. Downloaded on 4/24/2025 4:15:25 AM.
This article is licensed under a Creative Commons Attribution-NonCommercial 3.0 Unported Licence.

Chemical Science Accepted Manuscript

View Article Online
DOI: 10.1039/D5SC01269D

To further confirm the structure of organometallic intermediates linked by C−Cu−Br−Cu−C and C−Cu−C bonds, bond-resolving (BR) nc-AFM experiment was performed using a CO-functionalized probe.[44] A 6-membered nanoring containing two C−Cu−C and four C−Cu−Br−Cu−C bonds is shown in Fig. 2f-g. According to the BR nc-AFM image, the C−Cu−C bond exhibits as an uniform and continuous line and the Br atom presents as a bright protrusion in BR nc-AFM image, thus in excellent agreement with previous reports.[38, 45-47] In addition, the structural model optimized by DFT calculations matches well with the corresponding nc-AFM image (Fig. 2h). We note that, similar as the case in Fig. 2d, the pyridine moiety and the central phenyl appear darker than the phenanthrene backbone because they bend to the Cu(111) surface driven by the strong interaction between pyridine moiety and the substrate (Fig. S9).

On the basis of the coexistence during annealing-stimulated transformation of C−Cu−Br−Cu−C and C−Cu−C bonded organometallic intermediates, we confirm that the unusual C−Cu−Br−Cu−C motif is the precursor state of C−Cu−C bond, thus filling the blank of the mechanism between C−X dissociation and C−Cu−C generation in on-surface Ullmann coupling reaction. Interestingly, a few nanorings containing Cu−Br−Cu bonds with a smaller angle where Br is further away from the ring center was occasionally observed in experiments (Fig. S11). In this case, the Br atom is leaving the nanoring but still grasped by the Cu coordination interaction, which might be a metastable transition or intermediate states of the transformation process between C−Cu−Br−Cu−C and C−Cu−C motifs.

The C−Cu−Br−Cu−C species completely transformed into the C−Cu−C linked chain at 353 K, in which monomer units align in a *trans*-configuration (Fig. S12). This is opposite as the case of C−Cu−Br−Cu−C linked nanorings, where the neighboring monomers are connected with a *cis*-configuration. We calculated the energy of both *trans*- and *cis*-structures of C−Cu−Br−Cu−C/C−Cu−C organometallic species on Cu(111) and confirm that a *cis*-configuration is energetically more favorable for the C−Cu−Br−Cu−C bonded intermediate while a *trans*-configuration is energetically more favorable for the C−Cu−C bonded intermediate (Fig. S13), in good agreement with experiments. Further annealing at a higher temperature of 413 K resulted in the dissociation of C−Cu−C bonds, but C−C covalent bonds were only occasionally observed due to the strong steric hindrance (Fig. S14). The dominating products are debrominated monomers and they aggregate through Br···H hydrogen bonding (Fig. S15).[39]

Open Access Article. Published on 21 April 2025. Downloaded on 4/24/2025 4:15:25 AM.
This article is licensed under a Creative Commons Attribution-NonCommercial 3.0 Unported Licence.

Chemical Science Accepted Manuscript

View Article Online
DOI: 10.1039/D5SC01269D

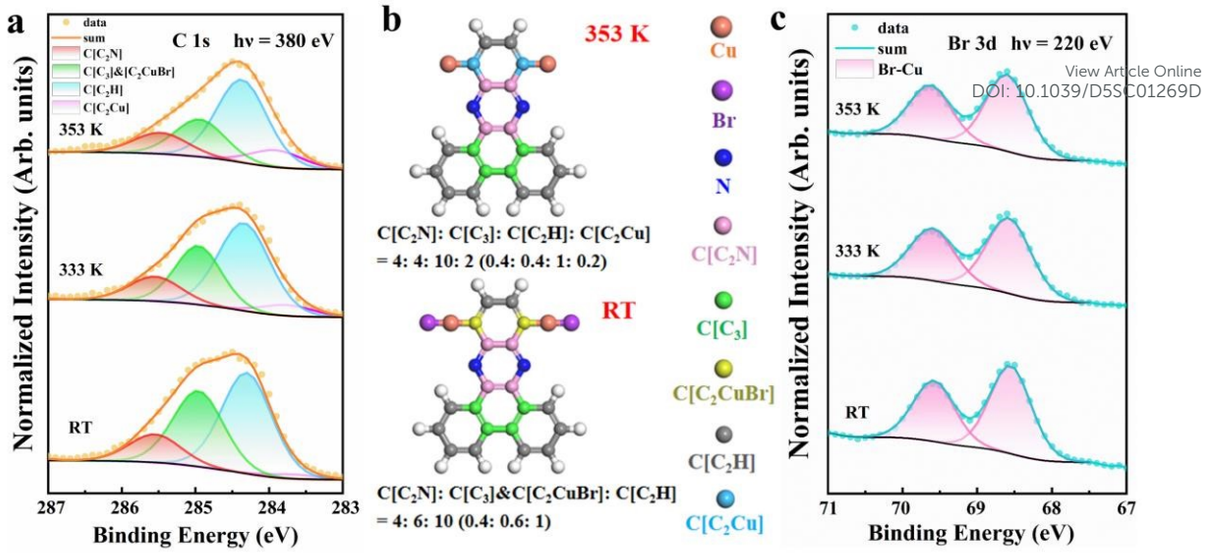

Fig. 3. SRPE spectra C 1s and of Br 3d showing the structural evolution of DBP-Br on the Cu(111) surface. (a) C 1s SRPE spectra of DBP-Br on Cu(111) recorded by annealing the sample at different temperatures. Circular marks represent original experimental data and solid lines represent the fitting. (b) Structural models of respective major product at RT and 353 K. Different atoms are depicted by different colors to illustrate their chemical environments. The ideal ratios of different C atoms as derived from the chemical structures are shown on the below. (c) Br 3d SRPE spectra of DBP-Br on Cu(111) recorded by annealing the sample at different temperatures.

The whole reaction process and further product confirmation in each reaction step are monitored by synchrotron radiation photoemission spectroscopy (SRPES) experiments. As shown in Fig. 3a, by fitting the original experimental data, four C species are identified at different temperatures. Based on the electronegativity of atoms linking the carbon and according to numerous previous works,[48-50] the order of binding energy (BE) of C 1s should be C[C_2N] (285.5 eV) > C[C_3]&C[C_2CuBr] (285.0 eV) > C[C_2H] (284.4 eV) > C[C_2Cu] (283.9 eV), as presented by red, green, blue, and purple lines, respectively (Fig. 3a). We note that because Br atom is a strong electron-withdrawing group, which significantly attracts the electron of Cu atom, the electron donation from Cu to C is suppressed (Fig. S16). Therefore, the BE of C[C_2CuBr] is close to that of C[C_3]. We thus consider the two types of carbons as a same component in the spectra fitting. At RT, the ratio of C[C_2N]: C[C_3]&C[C_2CuBr]: C[C_2H]=0.35: 0.6: 1 obtained from the experimental results, is very close to the ideal value derived from the chemical model of C−Cu−Br−Cu−C bonded nanoring (Fig. 3b). Importantly, this experimental fact provides a strong evidence for the structure assignment of C−Cu−Br−Cu−C, because the formation of other possible structures linked by C−$(Cu)_n$−C (n=2, 3) should give rise to the appearance of C[C_2Cu] signal at a low BE,[49, 51] which is absent in our experiments. Annealing to 333 K leads to the appearance of the signal of C[C_2Cu] in C 1s and the intensity decrease of C[C_2CuBr], indicating the transformation from C−Cu−Br−Cu−C to C−Cu−C was activated at this temperature, also in

Open Access Article. Published on 21 April 2025. Downloaded on 4/24/2025 4:15:25 AM.
This article is licensed under a Creative Commons Attribution-NonCommercial 3.0 Unported Licence.

Chemical Science Accepted Manuscript

good agreement with STM observations. The ratio of the four components changed into C[C_2N]: C[C_3]&[C_2CuBr]: C[C_2H]: C[C_2Cu] = 0.36: 0.4: 1: 0.2 upon further annealing at 353 K, matching well with the ideal stoichiometric value of the C−Cu−C linked product (0.4: 0.4: 1: 0.2). This in turn indicates a complete transformation from C−Cu−Br−Cu−C to C−Cu−C intermediates at 353 K, further supporting the associated STM results.

View Article Online
DOI: 10.1039/D5SC01269D

On the other hand, only one kind of Br species was identified in Br 3d spectra (Fig. 3c), featuring a spin−orbit doublet Br $3d_{3/2}$ and $3d_{5/2}$ with the BE of 69.7 and 68.6 eV, respectively.[52-54] This is because Br adatoms on Cu(111) generated by C−Br and C−Cu−Br−Cu−C dissociation have a similar chemical environment as the Br atoms in C−Cu−Br−Cu−C bond. In both cases, Cu atoms interact with and donate electrons to the linked Br atoms, although one kind of Cu is generated from Cu(111) surface and the other corresponds to the trapped Cu adatom by the molecules.

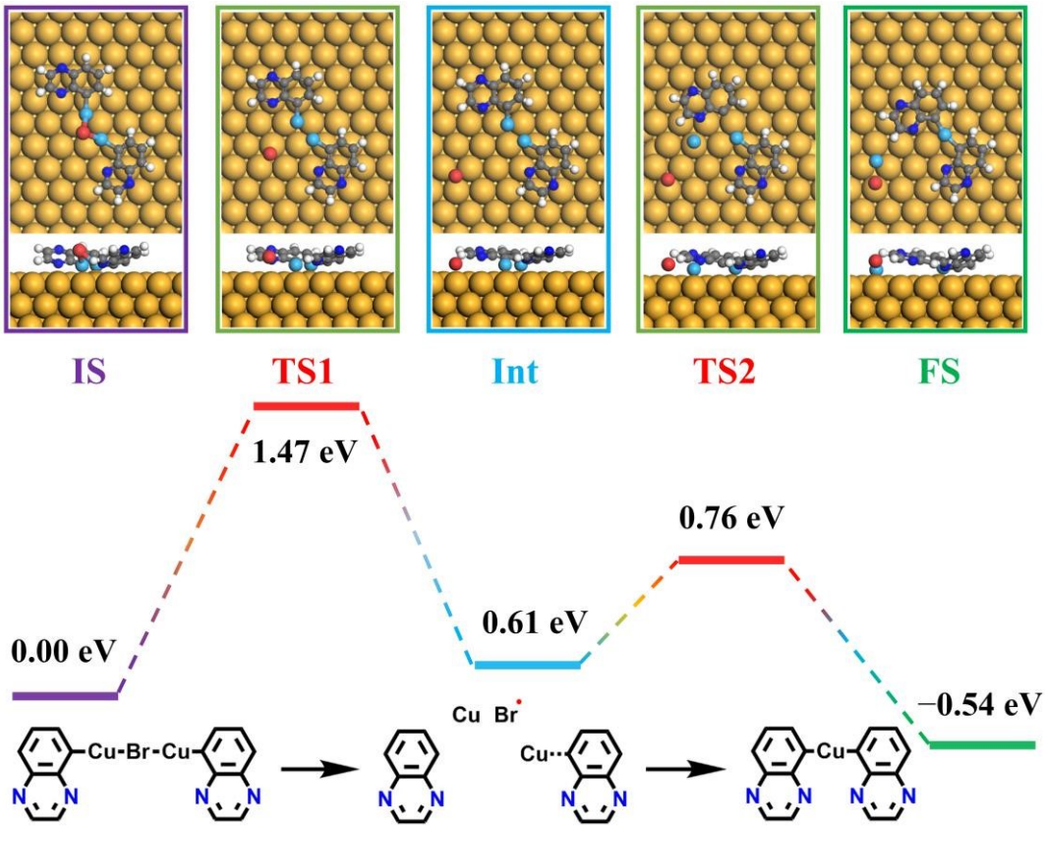

Fig. 4. DFT calculated structural transformation from C−Cu−Br−Cu−C to C−Cu−C bonded intermediates on Cu(111). Reaction pathway and energy profile in each step are presented.

To elucidate an atomistic understanding of the transformation process from C−Cu−Br−Cu−C to C−Cu−C bonds on the Cu(111) surface, we utilized climbing images nudged elastic band (CI-NEB) to calculate the reaction pathway.[55, 56] To balance the computational cost and accuracy, the structure of DBP unit is represented by a quinoxaline unit. The reaction path barrier diagram calculated by DFT is shown in Fig. 4. The initial reaction state (IS) shows that two quinoxaline units are connected by the C−Cu−Br−Cu−C bond adsorbed on Cu(111). In the next step, one Br atom leaves from the C−Cu−Br−Cu−C bond, by going

Open Access Article. Published on 21 April 2025. Downloaded on 4/24/2025 4:15:25 AM.
This article is licensed under a Creative Commons Attribution-NonCommercial 3.0 Unported Licence.

Chemical Science Accepted Manuscript

View Article Online
DOI: 10.1039/D5SC01269D

across a reasonable energy barrier (1.47 eV; TS1) to the intermediate state (0.61 eV; Int). Further, one Cu atom on one quinoxaline unit gradually leaves, and the quinoxaline unit moves toward another quinoxaline unit to form a more stable C−Cu−C bonded structure (−0.54 eV; FS), crossing a relatively low energy barrier (0.76 eV; TS2). The whole reaction undergoes an exothermic path, indicating that the transition from C−Cu−Br−Cu−C to C−Cu−C bonds is irreversible.

To our knowledge, such C−Cu−Br−Cu−C organometallic intermediates have not been reported in on-surface synthesis. Although the introduction of N atoms into the precursor molecule might be an indispensable factor for the formation of C−Cu−Br−Cu−C intermediates, it is not the only decisive parameter because such intermediate has never been observed via on-surface synthesis of other N-doped of aryl halides.[57-59] Therefore, we propose that the relative position of N atoms together with the special molecular backbone, as well as the formation of thermodynamically stable nanorings[60, 61] may also induce the generation of C−Cu−Br−Cu−C organometallic intermediates, by improving the stability and elongating the lifetime of C−Cu−Br−Cu−C intermediates. Note that the former determines the molecular adsorption geometry and steric hindrance effect, which is closely related to the substrate−molecule interaction and charge transfer (Fig. S16),[62-66] thus associating with the formation barrier and structural stability of the C−Cu−Br−Cu−C intermediates. In addition, previous studies reported that C–Cu–C has been formed at RT,[67, 68] whereas in this work, C–Cu–Br–Cu–C linked ring structure is observed at RT, implying that the formation of the nanorings provide a further stability to the system. Further studies will focus on how the precursor structure influences on the formation of the C−Cu−Br−Cu−C bonded intermediates by tuning parameters including the position of nitrogen substitution, length and shape of molecular backbone, charge transfer amount (as determined by ionization energy),[63] and ring tension, by designing more structurally similar precursors.

Conclusions

In summary, we report an unusual C−Cu−Br−Cu−C bonded intermediate in Ullmann coupling reaction of DBP-Br on Cu(111), forming high-yield N-doped nanorings. The topology of nanorings can be well tuned by changing the coverage of precursors on the surface. By careful inspection of structural transformation upon sample annealing, the C−Cu−Br−Cu−C motif is confirmed to be the precursor state of conventional C−Cu−C intermediate in on-surface Ullmann coupling. The structural validation is offered by the combination of STM, nc-AFM, SRPES, and DFT calculations. We propose that the formation of C−Cu−Br−Cu−C bonded nanorings is attributed to the synergy of multiple factors, including molecular adsorption geometry, molecule−substrate interaction, and charger transfer, as well as the stabilizing effect of the nanoring. These factors together contribute to a longer lifetime of the otherwise unstable C−Cu−Br−Cu−C intermediate. The visualization of an intermediate between C−X dissociation and C−Cu−C formation in this work extends the diversity of organometallic intermediates of Ullmann coupling on metal

Open Access Article. Published on 21 April 2025. Downloaded on 4/24/2025 4:15:25 AM.
This article is licensed under a Creative Commons Attribution-NonCommercial 3.0 Unported Licence.

Chemical Science Accepted Manuscript

surfaces. Notably, the C−Cu−Br−Cu−C intermediate is similar as the Cu(III) species proposed in solution-phase Ullmann coupling (Scheme 1c). However, in the C−Cu−Br−Cu−C intermediate reported in this work, Cu holds a valence state between +1 and +2, different from +3 of the similar Cu(III) intermediate in Cu(I)-Cu(III) ionic mechanism in solution. In turn, the mechanism rationalized in this work may also reasonably interpret the reaction pathway in Ni- and Pd-catalyzed Ullmann coupling reactions in addition to Cu-catalyzed systems in solution, since the associated intermediates hold the most common valence state (+1 or +2) of Ni and Pd. We thus propose a possibility that the C−M−Br−M−C intermediate might exist in conventional solution-phase metal-catalyzed Ullmann couplings, although the detailed mechanism is likely different from that on surface. This work opens a new avenue for revisiting the reaction mechanisms of Ullmann coupling both on surface and in solution.

View Article Online
DOI: 10.1039/D5SC01269D

Open Access Article. Published on 21 April 2025. Downloaded on 4/24/2025 4:15:25 AM.
This article is licensed under a Creative Commons Attribution-NonCommercial 3.0 Unported Licence.

Data availability

Experimental details and additional results can be found in the ESI.† All other data will be available on request.

Author contributions

X. M. conceived the project and designed the experiments. X. Z., L. L. and Z. Z. conducted the STM experiments under the supervision of T. W. and X. M.. X. Z. performed theoretical studies. X. Z., T. Q. and J. H. performed SRPES experiments under the supervision of J. Z.. T. W. and L. L. carried out the nc-AFM experiments. L. Y. synthesized precursor molecules. X. Z., L. L., Z. Z., T. W. and X. M. interpreted the results. X. Z., X. M., and T. W. co-wrote the manuscript with suggestions from all authors. All the authors discussed the results and commented on the manuscript.

Conflicts of interest

There are no conflicts to declare.

Acknowledgements

Financial support from the National Natural Science Foundation of China (22172055), the Strategic Priority Research Program of the Chinese Academy of Sciences (XDB1180000), the Science Fund for Distinguished Young Scholars of Guangdong Province (2023B1515040026), and the Natural Science Foundation of Guangdong Province (2022A1515011892). The authors thank Dr. Bingkai Yuan for nc-AFM characterization at the Vacuum Interconnected Nanotech Workstation (Nano-X), Suzhou Institute of Nano-Tech and Prof. Chao Zheng at Shanghai Institute of Organic Chemistry, CAS, for insightful discussions.

References

1 C. P. Delaney, E. Lin, Q. Huang, I. F. Yu, G. Rao, L. Tao, A. Jed, S. M. Fantasia, K. A. Püntener, R. D. Britt and J. F. Hartwig, *Science*, 2023, **381**, 1079-1085.

2 J. Feng, L.-L. Xi, C.-J. Lu and R.-R. Liu, *Chem. Soc. Rev.*, 2024, **53**, 9560-9581.

Chemical Science Accepted Manuscript

View Article Online
DOI: 10.1039/D5SC01269D

3 Laszlo Kurti and B. Czako, *Strategic applications of named reactions in organic synthesis*, Elsevier, 2005.
4 R. Akhtar, A. F. Zahoor, M. Irfan, T. H. Bokhari and A. ul Haq, *Chem. Pap.*, 2022, **76**, 7275-7293.
5 C. Sharma, A. K. Srivastava, D. Sharma and R. K. Joshi, *Org. Chem. Front*, 2022, **9**, 6252-6258.
6 O. Vyhivskyi, D. N. Laikov, A. V. Finko, D. A. Skvortsov, I. V. Zhirkina, V. A. Tafeenko, N. V. Zyk, A. G. Majouga and E. K. Beloglazkina, *J. Org. Chem*, 2020, **85**, 3160-3173.
7 F. Khan, M. Dlugosch, X. Liu and M. G. Banwell, *Acc. Chem. Res.*, 2018, **51**, 1784-1795.
8 B. Zhu, L.-K. Yan, L.-S. Yao, H. Ren, R.-H. Li, W. Guan and Z.-M. Su, *Chem. Commun.*, 2018, **54**, 7959-7962.
9 S. Clair and D. G. de Oteyza, *Chem. Rev.*, 2019, **119**, 4717-4776.
10 N. Pavliček, B. Schuler, S. Collazos, N. Moll, D. Pérez, E. Guitián, G. Meyer, D. Peña and L. Gross, *Nat. Chem.*, 2015, **7**, 623-628.
11 Q. Zhong, A. Ihle, S. Ahles, H. A. Wegner, A. Schirmeisen and D. Ebeling, *Nat. Chem.*, 2021, **13**, 1133-1139.
12 D. G. de Oteyza, P. Gorman, Y.-C. Chen, S. Wickenburg, A. Riss, D. J. Mowbray, G. Etkin, Z. Pedramrazi, H.-Z. Tsai, A. Rubio, M. F. Crommie and F. R. Fischer, *Science*, 2013, **340**, 1434-1437.
13 M. Di Giovannantonio, M. El Garah, J. Lipton-Duffin, V. Meunier, L. Cardenas, Y. Fagot Revurat, A. Cossaro, A. Verdini, D. F. Perepichka, F. Rosei and G. Contini, *ACS Nano*, 2013, **7**, 8190-8198.
14 B. Qie, Z. Wang, J. Jiang, Z. Zhang, P. H. Jacobse, J. Lu, X. Li, F. Liu, A. N. Alexandrova, S. G. Louie, M. F. Crommie and F. R. Fischer, *Science*, 2024, **384**, 895-901.
15 Z. Zeng, D. Guo, T. Wang, Q. Chen, A. Matěj, J. Huang, D. Han, Q. Xu, A. Zhao, P. Jelínek, D. G. de Oteyza, J.-S. McEwen and J. Zhu, *J. Am. Chem. Soc.*, 2022, **144**, 723-732.
16 J. Wang, K. Niu, H. Zhu, C. Xu, C. Deng, W. Zhao, P. Huang, H. Lin, D. Li, J. Rosen, P. Liu, F. Allegretti, J. V. Barth, B. Yang, J. Björk, Q. Li and L. Chi, *Nat. Commun.*, 2024, **15**, 3030.
17 W. Guo, J. Yin, Z. Xu, W. Li, Z. Peng, C. J. Weststrate, X. Yu, Y. He, Z. Cao, X. Wen, Y. Yang, K. Wu, Y. Li, J. W. Niemantsverdriet and X. Zhou, *Science*, 2022, **375**, 1188-1191.
18 G. Zhan, Z.-F. Cai, K. Strutyński, L. Yu, N. Herrmann, M. Martínez-Abadía, M. Melle-Franco, A. Mateo-Alonso and S. D. Feyter, *Nature*, 2022, **603**, 835-840.
19 D. Dettmann, M. Panighel, N. Preetha Genesh, G. Galeotti, O. MacLean, M. Farnesi Camellone, T. K. Johal, S. Fabris, C. Africh, D. F. Perepichka, F. Rosei and G. Contini, *J. Am. Chem. Soc.*, 2024, **146**, 24493-24502.
20 A. Kinikar, M. Di Giovannantonio, J. I. Urgel, K. Eimre, Z. Qiu, Y. Gu, E. Jin, A. Narita, X.-Y. Wang, K. Müllen, P. Ruffieux, C. A. Pignedoli and R. Fasel, *Nat. Synth.*, 2022, **1**, 289-296.
21 T. Wang and J. Zhu, *Surf. Sci. Rep.*, 2019, **74**, 97-140.
22 Z.-Y. Yi, Z.-C. Wang, R.-N. Li, Z.-H. Li, J.-J. Duan, X.-Q. Yang, Y.-Q. Wang, T. Chen, D. Wang and L.-J. Wan, *J. Am. Chem. Soc.*, 2024, **146**, 11342-11351.
23 C. Steiner, J. Gebhardt, M. Ammon, Z. Yang, A. Heidenreich, N. Hammer, A. Görling, M. Kivala and S. Maier, *Nat. Commun.*, 2017, **8**, 14765.
24 G. Galeotti, F. De Marchi, E. Hamzehpoor, O. MacLean, M. Rajeswara Rao, Y. Chen, L. V. Besteiro, D. Dettmann, L. Ferrari, F. Frezza, P. M. Sheverdyaeva, R. Liu, A. K. Kundu, P. Moras, M. Ebrahimi, M. C. Gallagher, F. Rosei, D. F. Perepichka and G. Contini, *Nat. Mater.*, 2020, **19**, 874-880.
25 J. Cai, P. Ruffieux, R. Jaafar, M. Bieri, T. Braun, S. Blankenburg, M. Muoth, A. P. Seitsonen, M. Saleh, X. Feng, K. Müllen and R. Fasel, *Nature*, 2010, **466**, 470-473.
26 L. Dong, P. N. Liu and N. Lin, *Acc. Chem. Res.*, 2015, **48**, 2765-2774.

Open Access Article. Published on 21 April 2025. Downloaded on 4/24/2025 4:15:25 AM.
This article is licensed under a Creative Commons Attribution-NonCommercial 3.0 Unported Licence.

Chemical Science Accepted Manuscript

View Article Online
DOI: 10.1039/D5SC01269D

27 M. Fritton, D. A. Duncan, P. S. Deimel, A. Rastgoo-Lahrood, F. Allegretti, J. V. Barth, W. M. Heckl, J. Björk and M. Lackinger, *J. Am. Chem. Soc.*, 2019, **141**, 4824-4832.
28 Q. Fan, L. Liu, J. Dai, T. Wang, H. Ju, J. Zhao, J. Kuttner, G. Hilt, J. M. Gottfried and J. Zhu, *ACS Nano*, 2018, **12**, 2267-2274.
29 A. Berdonces-Layunta, F. Schulz, F. Aguilar-Galindo, J. Lawrence, M. S. G. Mohammed, M. Muntwiler, J. Lobo-Checa, P. Liljeroth and D. G. de Oteyza, *ACS Nano*, 2021, **15**, 16552-16561.
30 W. Wang, X. Shi, S. Wang, M. A. Van Hove and N. Lin, *J. Am. Chem. Soc.*, 2011, **133**, 13264-13267.
31 Q. Fan, C. Wang, L. Liu, Y. Han, J. Zhao, J. Zhu, J. Kuttner, G. Hilt and J. M. Gottfried, *J. Phys. Chem. C*, 2014, **118**, 13018-13025.
32 Q. Fan, T. Wang, L. Liu, J. Zhao, J. Zhu and J. M. Gottfried, *J. Chem. Phys.*, 2015, **142**, 101906.
33 R. Giri, A. Brusoe, K. Troshin, J. Y. Wang, M. Font and J. F. Hartwig, *J. Am. Chem. Soc.*, 2018, **140**, 793-806.
34 S. Perveen, S. Zhang, L. Wang, P. Song, Y. Ouyang, J. Jiao, X.-H. Duan and P. Li, *Angew. Chem. Int. Ed.*, 2022, **61**, e202212108.
35 Q. Yang, Y. Zhao and D. Ma, *Org. Process Res. Dev.*, 2022, **26**, 1690-1750.
36 C. K. Krug, D. Nieckarz, Q. Fan, P. Szabelski and J. M. Gottfried, *Chem. Eur. J*, 2020, **26**, 7647-7656.
37 F. Xiang, A. Gemeinhardt and M. A. Schneider, *ACS Nano*, 2018, **12**, 1203-1210.
38 S. Zint, D. Ebeling, T. Schlöder, S. Ahles, D. Mollenhauer, H. A. Wegner and A. Schirmeisen, *ACS Nano*, 2017, **11**, 4183-4190.
39 Y. Lin, Z. Huang, X. Wen, W. Rong, Z. Peng, M. Diao, L. Xing, J. Dai, X. Zhou and K. Wu, *ACS Nano*, 2020, **14**, 17134-17141.
40 D.-Y. Li, Y. Wang, X.-Y. Hou, Y.-T. Ren, L.-X. Kang, F.-H. Xue, Y.-C. Zhu, J.-W. Liu, M. Liu, X.-Q. Shi, X. Qiu and P.-N. Liu, *Angew. Chem. Int. Ed.*, 2022, **61**, e202117714.
41 Y.-Q. Zhang, M. Paszkiewicz, P. Du, L. Zhang, T. Lin, Z. Chen, S. Klyatskaya, M. Ruben, A. P. Seitsonen, J. V. Barth and F. Klappenberger, *Nat. Chem.*, 2018, **10**, 296-304.
42 T. Wang, Q. Fan, L. Feng, Z. Tao, J. Huang, H. Ju, Q. Xu, S. Hu and J. Zhu, *ChemPhysChem*, 2017, **18**, 3329-3333.
43 C. Fan, B. Sun, Z. Li, J. Shi, T. Lin, J. Fan and Z. Shi, *Angew. Chem. Int. Ed.*, 2021, **60**, 13896-13899.
44 L. Gross, F. Mohn, N. Moll, P. Liljeroth and G. Meyer, *Science*, 2009, **325**, 1110-1114.
45 Q. Li, B. Yang, J. Björk, Q. Zhong, H. Ju, J. Zhang, N. Cao, Z. Shi, H. Zhang, D. Ebeling, A. Schirmeisen, J. Zhu and L. Chi, *J. Am. Chem. Soc.*, 2018, **140**, 6076-6082.
46 M. Liu, S. Li, J. Zhou, Z. Zha, J. Pan, X. Li, J. Zhang, Z. Liu, Y. Li and X. Qiu, *ACS Nano*, 2018, **12**, 12612-12618.
47 M. Telychko, J. Su, A. Gallardo, Y. Gu, J. I. Mendieta-Moreno, D. Qi, A. Tadich, S. Song, P. Lyu, Z. Qiu, H. Fang, M. J. Koh, J. Wu, P. Jelínek and J. Lu, *Angew. Chem. Int. Ed.*, 2019, **58**, 18591-18597.
48 D. Han, H. Ding, J. Xiong, T. Qin, X. Cheng, J. Hu, Q. Xu and J. Zhu, *ACS Nano*, 2024, **18**, 28946-28955.
49 T. Qin, D. Guo, J. Xiong, X. Li, L. Hu, W. Yang, Z. Chen, Y. Wu, H. Ding, J. Hu, Q. Xu, T. Wang and J. Zhu, *Angew. Chem. Int. Ed.*, 2023, **62**, e202306368.
50 M. Tenorio, C. Moreno, M. Vilas-Varela, J. Castro-Esteban, P. Febrer, M. Pruneda, D. Peña and A. Mugarza, *Small Methods*, 2024, **8**, 2300768.
51 R. Gutzler, L. Cardenas, J. Lipton-Duffin, M. El Garah, L. E. Dinca, C. E. Szakacs, C. Fu, M. Gallagher, M. Vondráček, M. Rybachuk, D. F. Perepichka and F. Rosei, *Nanoscale*, 2014, **6**, 2660-2668.
52 J. Hu, Z. Liang, H. Wang, H. Zhang, C. Huang, L. Xie, Z. Li, Z. Jiang, H. Huang and F. Song, *Appl.*

Open Access Article. Published on 21 April 2025. Downloaded on 4/24/2025 4:15:25 AM.
This article is licensed under a Creative Commons Attribution-NonCommercial 3.0 Unported Licence.

Chemical Science Accepted Manuscript

Surf. Sci., 2021, **566**, 150663.
53 D. Peyrot, M. G. Silly and F. Silly, *J. Phys. Chem. C*, 2017, **121**, 26815-26821.
54 H. Wang, Y. Wang, C. Zheng, P. Wang, Z. Hu and H.-Y. Gao, *J. Phys. Chem. Lett.*, 2024, **15**, 10535-10543.
55 J. Björk, *J. Phys.: Condens. Matter*, 2016, **28**, 083002.
56 G. Henkelman, B. P. Uberuaga and H. Jónsson, *J. Chem. Phys.*, 2000, **113**, 9901-9904.
57 L. Grill and S. Hecht, *Nat. Chem.*, 2020, **12**, 115-130.
58 H. Jiang, J. Lu, F. Zheng, Z. Zhu, Y. Yan and Q. Sun, *Chem. Commun.*, 2023, **59**, 8067-8070.
59 J. Xu, S. Xing, J. Hu and Z. Shi, *Commun. Chem.*, 2024, **7**, 40.
60 Q. Fan, T. Wang, J. Dai, J. Kuttner, G. Hilt, J. M. Gottfried and J. Zhu, *ACS Nano*, 2017, **11**, 5070-5079.
61 C. K. Krug, Q. Fan, F. Fillsack, J. Glowatzki, N. Trebel, L. J. Heuplick, T. Koehler and J. M. Gottfried, *Chem. Commun.*, 2018, **54**, 9741-9744.
62 M. Hollerer, D. Lüftner, P. Hurdax, T. Ules, S. Soubatch, F. S. Tautz, G. Koller, P. Puschnig, M. Sterrer and M. G. Ramsey, *ACS Nano*, 2017, **11**, 6252-6260.
63 T. Wang, A. Berdonces-Layunta, N. Friedrich, M. Vilas-Varela, J. P. Calupitan, J. I. Pascual, D. Peña, D. Casanova, M. Corso and D. G. de Oteyza, *J. Am. Chem. Soc.*, 2022, **144**, 4522-4529.
64 J. Xu, X. Zhu, S. Tan, Y. Zhang, B. Li, Y. Tian, H. Shan, X. Cui, A. Zhao, Z. Dong, J. Yang, Y. Luo, B. Wang and J. G. Hou, *Science*, 2021, **371**, 818-822.
65 J. Ren, M. Koy, H. Osthues, B. S. Lammers, C. Gutheil, M. Nyenhuis, Q. Zheng, Y. Xiao, L. Huang, A. Nalop, Q. Dai, H.-J. Gao, H. Mönig, N. L. Doltsinis, H. Fuchs and F. Glorius, *Nat. Chem.*, 2023, **15**, 1737-1744.
66 G. Wang, A. Rühling, S. Amirjalayer, M. Knor, J. B. Ernst, C. Richter, H.-J. Gao, A. Timmer, H.-Y. Gao, N. L. Doltsinis, F. Glorius and H. Fuchs, *Nat. Chem.*, 2017, **9**, 152-156.
67 S. Sun, B. Li, B. Fu, Z. Ruan, H. Zhang, W. Xiong, Y. Zhang, G. Niu, J. Lu, X. Zuo, L. Gao and J. Cai, *Chin. Chem. Lett.*, 2022, **33**, 5142-5146.
68 J. P. Calupitan, T. Wang, A. Pérez Paz, B. Álvarez, A. Berdonces-Layunta, P. Angulo-Portugal, R. Castrillo-Bodero, F. Schiller, D. Peña, M. Corso, D. Pérez and D. G. de Oteyza, *J. Phys. Chem. Lett.*, 2023, **14**, 947-953.

View Article Online
DOI: 10.1039/D5SC01269D
Open Access Article. Published on 21 April 2025. Downloaded on 4/24/2025 4:15:25 AM.
This article is licensed under a Creative Commons Attribution-NonCommercial 3.0 Unported Licence.
Chemical Science Accepted Manuscript

View Article Online
DOI: 10.1039/D5SC01269D

Data availability

Experimental details and additional results can be found in the ESI.† All other data will be available on request.

Open Access Article. Published on 21 April 2025. Downloaded on 4/24/2025 4:15:25 AM.
This article is licensed under a Creative Commons Attribution-NonCommercial 3.0 Unported Licence.

Chemical Science Accepted Manuscript